

Zero-Stress Optic Glass without Lead

M. Guignard, L. Albrecht, and J. W. Zwanziger*

Department of Chemistry and Institute for Research in Materials, Dalhousie University,
Halifax NS B3H 4J3, Canada

Received September 15, 2006. Revised Manuscript Received November 8, 2006

By comparing data on a variety of examples, an empirical correlation for the photoelastic response of simple metal oxides is discovered and used to predict new families of zero-stress optic glasses. The birefringence induced by uniaxial stress on glass is found to correlate well with the ratio of the metal oxygen bond metallicity to the metal coordination number; the metallicity itself is quantified through the metal oxygen bond length. This correlation was obtained by consideration of the stress optic response of a number of oxide crystals, obtained both from the literature when possible and also from first principles calculations. The correlation obtained provides a simple rule for choosing the composition of oxide glass so as to minimize the stress optic response; this rule is shown to agree with known data on lead oxide glasses and to predict the existence of previously unknown lead-free, zero-stress optic glasses. These glasses were then synthesized, tested, and shown to give the predicted response.

1. Introduction

Glass is optically isotropic, but when stress is applied, this symmetry is broken and glass usually becomes birefringent. Several remarkable glass compositions are known for which the birefringence is zero even in the presence of anisotropic stress; these include high contents of lead, thallium, or bismuth oxide. Such glasses are known as zero-stress optic materials and are key components in a variety of products, including optical research instruments, rear projection televisions, and liquid crystal on silicon projection systems. The origin of the zero-stress optic response is not understood, and recent environmental regulations forbidding the use of lead in many products has increased the urgency to understand this effect and discover suitable replacements. We have derived a relationship between atomic bonding and the stress optic response, which we present here along with calculations confirming this proposal. Most importantly, the proposed relationship indicates a variety of alternatives to lead oxide; we have prepared tin and antimony oxide-containing glasses and show that they behave analogously to high-lead glasses and thus we demonstrate new families of lead-free, zero-stress optic glasses.

The optical isotropy of glass means that its index of refraction is the same in all directions. When a symmetry-breaking perturbation is applied, such as uniaxial compressive or tensile stress, the isotropy is broken and the glass becomes birefringent. For many optical applications, image quality is of course greatly degraded by even small amounts of birefringence, and such systems benefit substantially from zero-stress optic glasses. In zero-stress optic glass, the birefringence is zero even in the presence of anisotropic stress loads. The compositional dependence of the birefringence is striking. The standard glass formers, such as SiO₂, B₂O₃, and P₂O₅, exhibit relatively large positive birefringence in

the presence of tensile stress. As these materials are modified with oxides such as Na₂O or BaO, the birefringence decreases for a given stress load. Lead oxide, PbO, is remarkable in that the addition of PbO reduces the birefringence all the way to zero and then to negative values at high content.¹ As noted, zero-stress optic compositions are of particular technological interest, but only a few additives are known to confer this behavior, in particular PbO, and also Bi₂O₃ and Ti₂O.^{2,3} All are heavy, expensive, and difficult to recycle and/or highly toxic. It is of considerable interest to understand the compositional dependence of the birefringence and to identify replacements with more benign environmental impact.

Typically, the index of refraction changes from the unstressed value both in the stress direction and orthogonal to it (Figure 1), usually with a greater change in the stress direction. More precisely, the birefringence is characterized by the stress optic coefficient C , which in the standard glass formers is positive. The stress optic coefficient C is defined through the relation

$$\delta = Cl\sigma \quad (1)$$

where δ is the optical path length difference for light polarization along the stress axis and that orthogonal to it (that is, the birefringence), l is the sample thickness, and σ is the applied uniaxial stress (Figure 1). For many glasses, C has magnitude 1–10 Brewster, where the unit of Brewster is $1 \times 10^{-12} \text{ Pa}^{-1}$. The effect is easy to see visually: by holding a piece of glass between crossed polarizers and squeezing with one's thumbs, the induced birefringence is clearly visible (Figure 2).

The stress optic coefficient C is a special case of the photoelastic response of solid matter. In general, the pho-

(1) Pockels, F. *Ann. Phys.* **1902**, *7*, 745–769.

(2) Rabukhin, A. I.; Belousova, G. V. *Glass Ceram.* **1992**, *49*, 458–462.

(3) Tashiro, M. *J. Soc. Glass Technol.* **1957**, *40*, 353T–362T.

* Corresponding author. E-mail: jzwanzig@dal.ca.

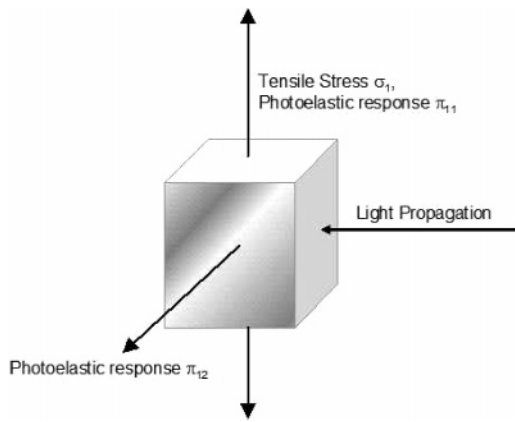


Figure 1. Geometry of the photoelastic response. Uniaxial stress σ_1 applied to the sample changes its dielectric response in both the stress direction (π_{11}) and in the orthogonal direction (π_{12}); the resulting birefringence is proportional to the difference $\pi_{11} - \pi_{12}$.

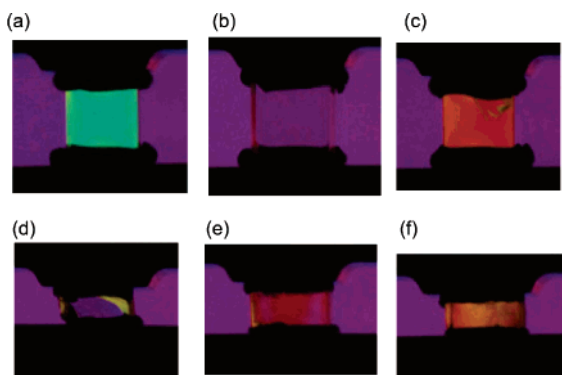


Figure 2. Induced birefringence in glass. In each frame, a glass sample is shown under uniaxial compressive stress, illuminated by polarized light and viewed through a quarter wave plate. Birefringence in this arrangement is indicated by a different color of the glass sample as compared to the background. The top row shows three Schott glass samples of predominantly lead silicate composition, with (a) positive, (b) zero, and (c) negative stress optic response; the bottom row shows three tin phosphate glasses, with (d) slightly positive, (e) negative, and (f) very negative stress optic response.

photoelastic tensor describes the relationship between changes in the inverse of the dielectric constant and applied stress or strain. It is conventional in this field to denote the inverse of the dielectric tensor by B . The photoelastic tensor is then given in components by the equation (in Voigt notation⁴)

$$\Delta B_i = \sum_j \pi_{ij} \sigma_j = \sum_j p_{ij} e_j \quad (2)$$

where ΔB refers to the difference between the stressed and unstressed values. Here, π_{ij} is the photoelastic tensor related to stress σ_j , and p_{ij} is the photoelastic tensor related to strain e_j . Either stress or strain can be used as control variables, and in the small stress limit, the two forms of the photoelastic tensor are related to each other by contraction with the elastic compliance tensor. Equation 2 can be used to compute the birefringence in an isotropic material in a state of tensile stress, and from this it can be shown that

$$C = -\frac{n^3}{2}(\pi_{11} - \pi_{12}) \quad (3)$$

where n is the index of refraction of the unstressed solid.⁵

Theories of photoelastic effects in glass focus on the polarizability of different ions under uniaxial stress. Mueller was the first to propose a theory of photoelasticity, suggesting that the effect arises from two terms, one due to lattice distortions and one arising from the atomic polarizability.^{6,7} In this model, the lattice term always confers negative birefringence, but is also mass dependent. The atomic term gives a positive effect and dominates in light materials such as silica. Heavy additives such as lead oxide are conjectured to confer negative stress response due to the dominance of the lattice term that they induce. In applications of Mueller's model, particular emphasis has been placed on the polarizability of the oxide anions, as these are the dominant species.^{3,8,9} Recent ab initio studies have focused more attention on the properties of the chemical bonds,^{10,11} which we believe is the most fruitful approach. Unlike the approach of Mueller, a bond-centered approach simplifies the estimation of the effect different chemical structures will have on the bulk stress optic response.

The approach we have taken to this problem is to first consider the stress optic response of a variety of simple metal oxides, including both glass formers and typical additives. These data were assembled both from the literature and from first principles calculations. From the data, we then deduce an empirical correlation between the material structure and bonding and the stress optic response. This correlation proves to be predictive, and correctly gives the compositions in lead oxide glasses where the stress optic response vanishes. It also predicts new families of lead-free, zero-stress optic materials, which we then made and tested, confirming the predictions.

2. Methods

2.1. First Principles Calculations. Computational results were obtained through use of the ABINIT code.¹² This is a density functional theory approach to finding the energies of periodic solids, in which the valence electron wavefunctions are expanded in terms of planewaves, and the effect of the core electrons are approximated through the use of pseudopotentials. Troullier–Martins pseudopotentials were used,¹³ generated with the FHI98 package.¹⁴

The properties of each system were computed using the local density approximation (LDA) for the exchange and correlation functionals, and reciprocal space was sampled using a shifted

(4) Nye, J. F. *Physical Properties of Crystals*; Oxford Science Publications: Oxford, U.K., 1985.

(5) Varshneya, A. K. *Fundamentals of Inorganic Glasses*; Academic Press: San Diego, CA, 1994.
 (6) Mueller, H. *Physics* **1935**, *6*, 179–184.
 (7) Mueller, H. *J. Am. Ceram. Soc.* **1938**, *21*, 27–33.
 (8) Borelli, N. F.; Miller, R. A. *Appl. Opt.* **1968**, *7*, 745–750.
 (9) Matusita, K.; Yokota, R.; Kimijima, T.; Komatsu, T.; Ihara, C. *J. Am. Ceram. Soc.* **1984**, *67*, 261–265.
 (10) Donadio, D.; Bernasconi, M.; Tassone, F. *Phys. Rev. B* **2003**, *68*, 134202.
 (11) Donadio, D.; Bernasconi, M.; Tassone, F. *Phys. Rev. B* **2004**, *70*, 214205.
 (12) Gonze, X.; Beuken, J. M.; Caracas, R.; Detraux, F.; Fuchs, M.; Rignanese, G. M.; Sindic, L.; Verstraete, M.; Zerah, G.; Jollet, F.; Torrent, M.; Roy, M.; Mikami, M.; Ghosez, Ph.; Raty, J. Y.; Allan, D. C. *Comp. Mater. Sci.* **2002**, *25*, 478–492.
 (13) Troullier, N.; Martins, J. L. *Phys. Rev. B* **1991**, *43*, 1993–2006.
 (14) Fuchs, M.; Scheffler, M. *Comput. Phys. Commun.* **1999**, *119*, 67.

Monkhorst–Pack grid¹⁵ at a spacing of about 0.035 \AA^{-1} . The following general approach was used to compute the photoelastic tensors. First, for each system studied, the experimentally determined crystal structure was optimized such that no force on an atom exceeded $2 \times 10^{-5} \text{ Ha/Bohr}$. This led typically to a reduction in the unit-cell side lengths by several percent, as is usually found within the LDA model. Then, for the optimized structure, the elastic tensor and dielectric tensor were calculated. In both cases, ion positional relaxation was allowed for; the dielectric tensor was computed in the approximation of frequencies high compared to phonon modes but low compared to electronic excitations.

Once the elastic constants and dielectric constants were computed for the optimized structure, strain was applied to the unit cell and the atom positions were reoptimized (provided they were not on special positions) in order again to minimize forces. The dielectric tensor was then computed for the final strained structure. The dielectric tensors were then treated as matrices and inverted to derive the permittivity tensors, and the difference between the permittivity tensors of the strained and unstrained structures calculated in order to obtain the tensor ΔB . From this tensor and the strain, we derived the elements of the photoelastic tensor. The photoelastic tensor relating to stress was then computed by contraction with the compliance tensor.

2.2. Glass Preparation. Four tin silicate glasses were synthesized from silicon dioxide (SiO_2) and tin(II) oxide (SnO) with the chemical composition $(\text{SnO})_x(\text{SiO}_2)_{1-x}$, where $x = 40, 50, 55$, and 60 mol \% . The reagents were melted under an argon pressure of about 0.5 bar in a covered alumina crucible at $1500 \text{ }^\circ\text{C}$ for 30 min in an induction furnace. The liquid was then cooled to room temperature in the crucible by switching off the furnace. Crucibles were finally broken to take out yellowish glasses. As the cooling was slow, no residual mechanical stress was observed in these glasses through the polarimeter and no additional annealing was required.

Four phosphate glasses were synthesized from ammonium dihydrogen-phosphate ($\text{NH}_4\text{H}_2\text{PO}_4$) and tin(II) oxide with the chemical composition $(\text{SnO})_x(\text{P}_2\text{O}_5)_{1-x}$, where $x = 55, 60, 66$, and 75 mol \% . The reagents were melted under argon in an alumina crucible at $1050 \text{ }^\circ\text{C}$ for 30 min in a muffle furnace. Glasses were then obtained by pouring the liquid onto a brass plate at room temperature. They were then annealed at about $250 \text{ }^\circ\text{C}$ for 2 h in a muffle furnace and slowly cooled to room temperature ($1 \text{ }^\circ\text{C}/\text{min}$) to reduce residual mechanical stresses induced during the quenching. The tin oxidation state was determined in phosphate glasses using Mössbauer spectroscopy, which demonstrated that only a small amount of tin(IV) was present ($1\text{--}3 \text{ mol \%}$) in low tin content glasses, whereas its presence was undetectable at high tin content. For both tin silicate and phosphate glasses, chemical composition was checked using energy dispersive spectroscopy (EDS), coupled with scanning electron microscopy (SEM) observation. This analysis showed that the real composition differed from the nominal one by about 1 to 2 mol \% more tin in phosphate glasses. In tin silicates, EDS analysis showed some incorporation of aluminum from the crucible in the glasses. However, the molar ratio of Sn to Si was close to that expected, and we assumed that the substitution of silicon dioxide by tin(II) oxide is mainly responsible for the decrease of the photoelastic constant.

Two antimony borate glasses were synthesized from anhydrous boric oxide (B_2O_3) and antimony oxide (Sb_2O_3) with the chemical composition $(\text{Sb}_2\text{O}_3)_x(\text{B}_2\text{O}_3)_{1-x}$, where $x = 40$ and 50 mol \% . The reagents were melted in air in an alumina crucible at $1100 \text{ }^\circ\text{C}$ for 15 min in a muffle furnace. Glasses were then obtained by pouring

Table 1. Stress optic Coefficients for Simple Crystals^a

compd	$\langle C \rangle$ /Brewsters
MgO	4.03
BaO	9.39
TeO2	47.0
SnO2	7.47
PbS	243
SnO	-39.9
PbO	-3.83
HgO	-39.9

^a The stress optic coefficients were obtained by computing the full photoelastic tensor of each crystal using first-principles methods, isotropically averaging it, and then computing the stress optic coefficient using the averaged tensor elements and eq 3.

the liquid on a brass plate at room temperature and annealed at about $300 \text{ }^\circ\text{C}$ for 2 h in a muffle furnace.

To perform the photoelastic constant measurement, we cut glasses to obtain samples of about $10 \times 5 \times 5 \text{ mm}^3$ and polished two parallel sides.

2.3. Measurement of Stress Optic Coefficients. The photoelastic constant was measured using the Sénarmont or quarter-wave plate compensator method using a polarimeter (PS-100 Strainoptic).¹⁶ The light source was two 8 W tungsten halogen bulbs. The sample was strained such that its stress axes were at 45° to the polarizer axis. In the PS-100 polarimeter, the quarter-wave plate is fixed between the sample and the analyzer such that the fast axis of the plate is aligned with the polarizer axis. Under these conditions, extinction was obtained by rotating the analyzer by an angle of $\theta/2$, where θ is the phase difference between the extraordinary and the ordinary rays. The optical path length difference δ was then determined by the equation $\delta = \theta\lambda$, considering the wavelength λ of 565 nm for applied stresses in the range of 0 to about $13 \times 10^6 \text{ Pa}$ depending on the composition. The slope of the graph of δ as a function of σ was then used together with the defining relation $\delta = C\sigma$ and the sample thickness l to determine the stress optic coefficient C . To estimate the accuracy of our experiment using a white light source, we measured the photoelastic constant of three Schott commercial glasses for which C is known. We obtained photoelastic constants of $2.39, 0.58$, and -1.40 Brewsters for SF2, SF6, and SF59 glasses, respectively, which is in reasonable agreement with Schott values of $2.62, 0.65$, and -1.36 Brewsters for these glasses measured at the wavelength of 589 nm . Thus, the accuracy of our measurement is estimated at about $\pm 10\%$.

3. Results and Discussion

To generate a data set of the stress optic response of different crystal structures, we performed first principles calculations of the photoelastic tensors of a variety of simple oxides. In addition, the photoelastic response of many other relevant crystals can be obtained from the literature. The choice of which compounds to study was made on the basis of the need for simple but relevant crystal structures, the inclusion of both heavy metals that form covalent bonds and heavy metals that bond ionically, and the inclusion of at least one compound that is a glass former and a nonmetallic cation. Because the crystals studied have different structures, their photoelastic tensors have different forms. To compare them and make contact with isotropic glasses, we report in Table 1 the computed stress optic coefficients. These values were obtained by isotropically averaging the computed photoelastic

(15) Monkhorst, H. J.; Pack, J. D. *Phys. Rev. B* **1976**, *13*, 5188–5192.

(16) Jerrard, H. G. *J. Opt. Soc. Am.* **1948**, *38*, 35–59.

π tensors¹⁷ and then using eq 3. Table 1 shows that a range of C values are obtained, though what is of particular interest here is the sign of C . Note as well that whereas PbO gives a negative response, PbS is positive; these two compounds differ structurally in that the oxide has coordination number four, whereas the sulfide has coordination number six.

The results in Table 1 show that the stress optic response is not simply related to ion mass or oxide ion polarizability but rather is evidently related both to polarizability and structure. This finding is understandable because the effect depends on the way in which the full crystal responds to anisotropic stress. We considered several simple models that might capture this response, including the presence or absence of stereochemically active lone pairs on the cation centers and the covalency of the cation oxygen bonds. These models failed, however, to give a good correlation with the known and computed stress optic response in a wide variety of materials. We found that a model that combines the so-called bond metallicity with the crystal structure provides a good correlation with most of the known data.

Bond metallicity refers to the increase in s-p hybridization and reduced band gaps in materials; in a very wide selection of materials, including those considered here, it correlates well with the cation-anion bond length d .¹⁸ We conjecture that metallicity is important to describe the stress optic response, because high metallicity should correlate with polarizability both along and orthogonal to the bonds. In other words, as the bonds become less directional (more metallic), stress in a given direction may distort them both in the stress direction and that orthogonal to it. This non-directional character is needed in order to achieve $C = 0$, which will occur when $\pi_{11} = \pi_{12}$ (see eq 3). On the other hand, if the full crystal structure is characterized by large coordination numbers, as for example in PbS (rock salt structure), any stress will deform bonds both in the stress direction and that orthogonal to it; in this case, high metallicity will be overcome by the bulk isotropic response of the crystal. Thus we suggest that zero- or negative-stress optic response should be favored by high metallicity and low coordination numbers. We quantify this proposal by computing d/N_c , where d is the bond length (and correlates positively with metallicity) and N_c is the cation coordination number. The results are presented in Table 2, along with the sign of the stress optic coefficient for each case.

Table 2 shows that oxides with d/N_c values greater than 0.5 Å all confer negative stress optic response, whereas those with d/N_c less than 0.5 Å are all positive. The value $d/N_c \approx 0.5$ should thus correspond to a zero-stress optic material. The exact boundary value is probably slightly higher than 0.5, as we know that TeO₂ is a positive-stress optic response material. However, we are not proposing Table 2 as an exact, quantitative result, but rather as qualitative guide with reasonable predictive power. The correlation of Table 2 predicts a variety of possible zero- and negative-stress optic glasses, to be obtained by blending a glass former with one or more of the high d/N_c oxides. Moreover, because in this

Table 2. Cation–Anion Bond Length d , Cation Coordination Number N_c , and the Ratio d/N_c for a Variety of Materials, along with the Sign of the Stress Optic Coefficient C^a

compd	d (Å)	N_c	d/N_c (Å)	sign of C	source
HgO	2.067	2	1.03	–	calcd ^b
Tl ₂ O	2.517	3	0.84	–	expt ³
Sb ₂ O ₃	2.022	3	0.67	–	expt ^b
PbO	2.326	4	0.58	–	calcd, ^b expt ¹
SnO	2.224	4	0.56	–	calcd, ^b expt ^b
Bi ₂ O ₃	2.198	4	0.55	–	expt ²
TeO ₂	2.0	4	0.50	+	calcd ^b
ZnO	1.988	4	0.50	+	expt ⁹
PbS	2.967	6	0.49	+	calcd ^b
BaO	2.74	6	0.46	+	calcd, ^b expt ⁹
B ₂ O ₃	1.366	3	0.46	+	expt ⁹
GeO ₂	1.717	4	0.43	+	expt ²⁰
SiO ₂	1.609	4	0.40	+	expt ^{1,3,8}
P ₂ O ₅	1.5	4	0.38	+	expt ³
MgO	2.1085	6	0.35	+	calcd, ^b expt ³
SnO ₂	2.055	6	0.34	+	calcd ^b

^a The final column indicates how the sign of C was derived: “calcd” Means based on first-principles calculation in the crystal as in Table 1, and “expt” means based on the measured value for the compound added to typical glass formers. In the latter case, a negative sign is recorded if it is known that negative C can be achieved for the given additive at high enough loadings. References give data sources. ^b This work.

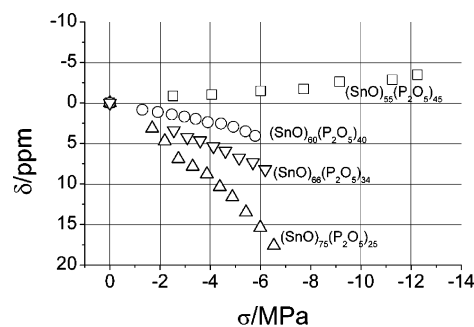


Figure 3. Birefringence as a function of compressive uniaxial stress in tin phosphate glasses, for different compositions. Compressive stress is by convention negative, and is plotted here in increasing magnitude; the birefringence axis was thus inverted as well. Because both axes are inverted, on the graph a positive slope still corresponds to a positive stress optic coefficient.

simple view the photoelastic response is determined primarily by the metal oxygen bonds, it should be sufficient to average the d/N_c values in a multicomponent glass in order to derive the expected response. In other words, Table 2 suggests the following rule to obtain a zero-stress optic glass

$$\sum_i x_i \left(\frac{d}{N_c} \right)_i \approx 0.5 \quad (4)$$

where the sum is over all components in the glass, x_i their mole fractions, and $(d/N_c)_i$ their d/N_c values. Using the data in Table 2 and eq 4, for example, lead silicate glass is predicted to have zero-stress optic coefficient for a mole fraction of 55% PbO, in reasonable agreement with the experimental value of about 50%.¹

We then used the approach of Table 2 and eq 4 to predict several new zero-stress optic glasses that do not use the traditional additives for this purpose. In particular, we prepared samples of tin(II) phosphate, tin(II) silicate, and antimony borate glasses. Data for the birefringence as a function of stress are shown in Figures 3–5. The stress optic coefficients for these glasses as functions of composition are

(17) Newnham, R. E. *Properties of Materials*; Oxford University Press: Oxford, U.K., 2005.

(18) Wemple, S. H. *J. Chem. Phys.* **1977**, *67*, 2151–2168.

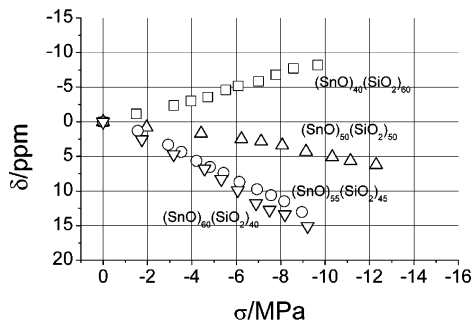


Figure 4. Birefringence as a function of compressive uniaxial stress in tin silicate glasses, for different compositions, as in Figure 3.

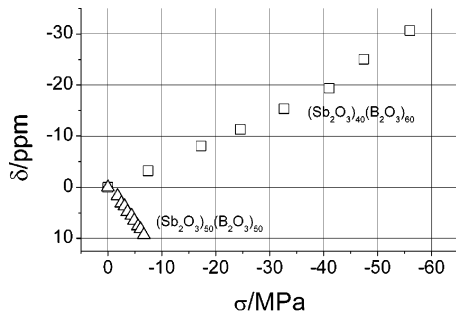


Figure 5. Birefringence as a function of compressive uniaxial stress in antimony borate glasses, for different compositions, as in Figure 3.

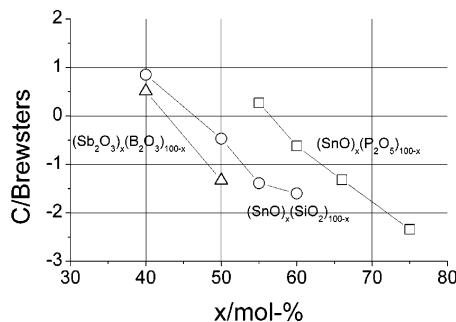


Figure 6. Stress optic coefficient C as a function of composition for several lead-free glass chemistries.

shown in Figure 6. Although only a few compositions were formulated, each shows positive response at low additive concentration and negative response at high concentration, with a smooth variation. Clearly, compositions exist in the intermediate regime with precisely zero-stress optic response. Furthermore, Figure 6 shows the trend predicted by eq 4. For example, less Sb_2O_3 is needed than tin(II) oxide to achieve $C = 0$, because Sb_2O_3 has a markedly higher d/N_c value than does, making it a more efficient additive in this application.

On the basis of the above model (eq 4), we predicted the mole fractions of additive necessary to achieve $C = 0$ to be 0.64, 0.64, and 0.20 for tin(II) phosphate, tin(II) silicate, and antimony borate, respectively. Figure 6 shows that these predictions are in only fair agreement with the data; interpolating our measurements to find $C = 0$ indicates that

additive fractions of 0.56, 0.47, and 0.43 would be necessary to achieve precisely $C = 0$. The antimony borate case is particularly far off, but notice that we have assumed a boron coordination number of three in making the prediction. Borate glasses are well-known to show variable boron coordination, with typically 3-fold coordination at low and high boron content and 4-fold coordination at intermediate levels. Antimony borate is no exception,¹⁹ and if we use a coordination number of 3.5 for boron instead of 3 in eq 4, the antimony borate glass is predicted to show $C = 0$ for an additive fraction of 0.39, in much better agreement with the data. In general, such details could always be included in using eq 4, but we typically refrain from doing so because the predictive power of this model lies in the very simple input used to generate broadly correct predictions about the stress optic response of glass.

Finally, in the case of ternary and higher glasses, eq 4 must be understood to include contributions from each component in the glass. The model posits that the bonds are all that matter in the response, so by accounting for them as suggested in eq 4, all relevant effects will be reflected. We will test this prediction in forthcoming work.

4. Conclusions

The primary conclusions of this work are the formulation of an empirical explanation for photoelastic response in oxide glasses and the demonstration of new families of lead-free, zero-stress optic materials (patent pending). The key element of the correlation is that the optical response is due to the chemical bonds. The aspects of the bonding that are important are the metallicity, to obtain polarizability both in the direction of and orthogonal to the bond, and low coordination number, so that the bonded unit may be deformed anisotropically by the stress. We captured these two elements in the empirical parameter d/N_c . From the parameter values for a variety of oxides, we could reproduce the known compositional behavior of the stress optic coefficient in lead silicates and predict that tin(II) glasses and antimony oxide glasses, among others, could also be zero-stress optic materials. We prepared these glasses and validated the prediction, thus discovering new families of lead-free, zero-stress optic glass.

Acknowledgment. We thank Andrew George of Dalhousie University for helping with the silicate glass syntheses and Paul MacInnis for assistance with software installation and maintenance. We thank the National Sciences and Engineering Council of Canada, the Canadian Foundation for Innovation, and the Canada Research Chairs program for financial support.

CM062208A

(19) Youngman, R. E.; Sen, S.; Cornelius, L. K.; Ellison, A. J. G. *Phys. Chem. Glasses* **2003**, *44*, 69–74.

(20) Rabukhin, A. I. *Glass Ceram.* **1994**, *51*, 353–359.